PNAS RESEARCH ARTICLE | NEUROSCIENCE

Hippocampal ripples signal contextually mediated episodic recall

John J. Sakon[a] and Michael J. Kahana[a,1]

Edited by Carol Barnes, The University of Arizona, Tucson, AZ; received January 28, 2022; accepted August 14, 2022

High-frequency oscillatory events, termed ripples, represent synchrony of neural activity in the brain. Recent evidence suggests that medial temporal lobe (MTL) ripples support memory retrieval. However, it is unclear if ripples signal the reinstatement of episodic memories. Analyzing electrophysiological MTL recordings from 245 neurosurgical participants performing episodic recall tasks, we find that the rate of hippocampal ripples rises just prior to the free recall of recently formed memories. This prerecall ripple effect (PRE) is stronger in the CA1 and CA3/dentate gyrus (CA3/DG) subfields of the hippocampus than the neighboring MTL regions entorhinal and parahippocampal cortex. PRE is also stronger prior to the retrieval of temporally and semantically clustered, as compared with unclustered, recalls, indicating the involvement of ripples in contextual reinstatement, which is a hallmark of episodic memory.

hippocampal ripples | episodic memory | contextual reinstatement | medial temporal lobe | intracranial EEG

Significance

High-frequency electrophysiological events in the medial temporal lobe (MTL)—known as ripples—have been linked to memory retrieval. Here, using electrophysiological recordings from neurosurgical patients performing free-recall tasks, we confirm that hippocampal ripples rise in rate just prior to word recall in humans. Notably, we see the highest ripple rates prior to recalls most likely achieved via contextual reinstatement, supporting hypotheses from rodent work that ripples reflect engagement of episodic memory mechanisms. We also find significantly more ripples prior to recall in hippocampal areas cornu ammonis region 1 and dentate gyrus than in nearby MTL cortical regions, uncovering a physiological correlate of successfully retrieved episodic memories.

Studies in rodents (1) and nonhuman primates (2, 3) have identified bursts of high-frequency oscillatory activity, known as ripples, in the hippocampus and surrounding medial temporal lobe (MTL) regions. These ripples reflect the coordinated activity of large neuronal ensembles in the hippocampus (4) and cortex (5). Experiments in animal models have linked ripples to consolidation and replay during quiescent and sleep states (1), and more recent work has linked them to awake behavior (6–10). Converging evidence from animal studies (10) and new examinations in humans support the hypothesis that hippocampal (11–14) or MTL cortical (15, 16) ripples signal upcoming memory retrieval.

Here, we ask whether ripples specifically signal the retrieval of episodic memories—those memories characterized by a "jump back in time" (17)—as reflected in behavioral evidence for the reinstatement of past contextual associations. For example, if you visited Kyoto, a future reminder of the city might lead to a reinstatement of the context of your trip, thereby spurring the retrieval of many memories associated with it (the taste of green tea in Uji, walking through the orange gates at Fushimi Inari, etc.). Contextual reinstatement plays a central role in models of episodic memory (18–20), and humans with amnestic disorders exhibit marked impairments in the behavioral markers of reinstatement (21). Considering the link between MTL ripples and retrieval, do ripples reflect contextual reinstatement and, consequently, episodic recall?

We answer this question by analyzing two intracranial electroencephalogram (iEEG) datasets of participants with electrodes implanted in hippocampal subfields CA1 or CA3/dentate gyrus (DG)—regions critical for episodic memory (22–24)—as well as neighboring entorhinal (ENT) or parahippocampal (PHC) cortices. Participants took part in at least one of two memory paradigms: delayed free recall of unrelated word lists (FR; 195 participants, 970 bipolar electrode pairs; Fig. 1*A*) and delayed free recall of categorized word lists (catFR; 126 participants with 76 of them also FR participants, 570 bipolar electrode pairs; see Fig. 4*A*). Free recall, in which participants study a list of sequentially presented items and subsequently attempt to recall them in any order, allows researchers to isolate the processes underlying episodic memory retrieval (25). Transitions between consecutively recalled items enable the identification of neural processes underlying contextual reinstatement, as they can reflect both semantic and temporal associations among studied items (19, 20, 26). By relating ripples to how these associations organize memory, we aim to determine whether ripples signal contextually mediated retrieval processes.

To detect ripples, we use an algorithm recently shown to isolate such high-frequency events in the human hippocampus during both memory encoding and retrieval (11) (*Materials and Methods*). Ripple peak frequencies (Fig. 1*C*), durations, spatial proximity, and rates (*SI Appendix*, Figs. 1 and 2) are similar to previous work (11, 12, 15). Anatomical localization of electrodes was performed by a combination of neuroradiologist labels and automated segmentation via separate processes for the hippocampal subfields (27) and the ENT and PHC cortices (28, 29).

Author affiliations: [a]Department of Psychology, University of Pennsylvania, Philadelphia, PA 19104

Author contributions: J.J.S. and M.J.K. designed research; J.J.S. performed research; J.J.S. analyzed data; and J.J.S. and M.J.K. wrote the paper.

The authors declare no competing interest.

This article is a PNAS Direct Submission.

[1]To whom correspondence may be addressed. Email: kahana@psych.upenn.edu.

This article contains supporting information online at https://www.pnas.org/lookup/suppl/doi:10.1073/pnas.2201657119/-/DCSupplemental.

Published September 26, 2022.

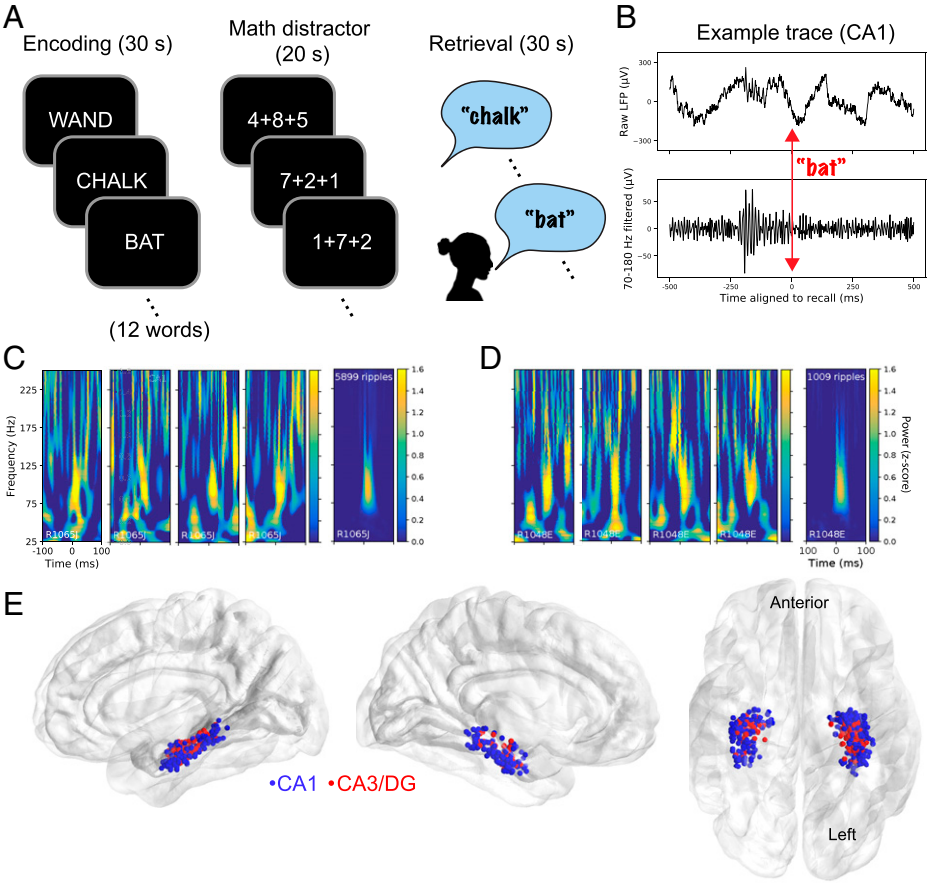

Fig. 1. Free-recall task and ripple details. (*A*) Each list of the free-recall task consists of an encoding period with 12 words presented sequentially, an arithmetic distractor, and a verbal free-recall phase. (*B*) Example hippocampal CA1 trace of raw (*Upper*) and Hamming band-pass-filtered (*Lower*) LFP aligned to the time of recall vocalization. Red indicates alignment to time of vocalization when the participant says "bat." (*C*) Example spectrograms of single ripples detected in CA1 for two participants, four from each. Each plot shows 100 ms before and after aligned to the start of a single ripple event. Anonymized participant codes are at the bottom of the figure in white. (*D*) Average spectrograms for all ripples across sessions in CA1 for the same two participants. (*E*) Localization of hippocampal CA1 and DG (CA3/DG) electrode pairs for all FR participants. From left to right: left sagittal, right sagittal, and inferior. Sagittal views are transparent for the hemisphere with plotted electrodes. CA1, $n = 335$ bipolar electrode pairs; CA3/DG, $n = 161$.

We partitioned our data into two halves: a first half for developing initial analyses, and a second half held out as a confirmatory dataset. We preregistered our hypotheses as well as the initial figures for the first half of the data on the Open Science Framework (https://osf.io/y5zwt). Therefore, for the main tests throughout the manuscript, we present two sets of statistics: 1) the significance of model coefficients on the held out half of data and 2) the significance of model coefficients on the full dataset (*Materials and Methods*).

The analyses detail three main findings. First, we establish the prerecall ripple effect (PRE), in which ripples occur just prior to the vocalization of freely recalled words. Next, we find that this effect is strongest in hippocampal subfields CA1 and CA3/DG. Finally, we show that the PRE shows the highest ripple rates on trials more likely to reinstate episodic information.

Results

The Prerecall Retrieval Effect (PRE). To elucidate the relation between ripples and recall, we align hippocampal recordings to the onset of each correct recall vocalization in the FR dataset. A raster plot for 10 example participants with hippocampal recordings illustrates when ripples occur with respect to these recalls, where each row is a recording from a single channel aligned to a correctly recalled word, and each dot represents the start time of a single ripple (Fig. 2*A*). The raster suggests that ripple rates rise several hundred milliseconds prior to vocalization onset, as shown in recent work (11, 12, 15).

Models of free recall posit separate mechanisms for recall initiation and subsequent retrieval transitions, with the former being driven by a persistent representation of items or context and the latter being driven by cue-dependent associative retrieval (25, 30). Recordings from hippocampal subfields CA1 and CA3/DG, averaged across all participants into peri-vocalization time histograms (PVTHs), reveal clear physiological evidence for this distinction. Specifically, cue-dependent recalls (i.e., those following the first response, or ≥second recalls) exhibit a sharp rise in ripples prior to word vocalization (Fig. 2*B*), which we term the PRE. In contrast, the first recall in each retrieval period does not show this same PRE (Fig. 2*B*).

Using a linear mixed-effects model to quantify this distinction, while accounting for both within-and between-participant variability (Eq. **1**), we find PRE to be significantly stronger for ≥second recalls compared to first recalls, an effect that appears in both CA1 (Fig. 2 *B*, *Left*) and CA3/DG (Fig. 2 *B*, *Right*). Further, PRE is statistically significant across participants for both CA1 and CA3/DG when looking at the rise in ripples compared to baseline rates for ≥second recalls (Fig. 2*C* and Eq. **2**).

We next ask whether PRE for ≥second recalls correlates with memory performance. Measuring the ripple rate of PRE averaged across correct recalls from a given list and correlating it with the number of recalls from that list, we find that participants show

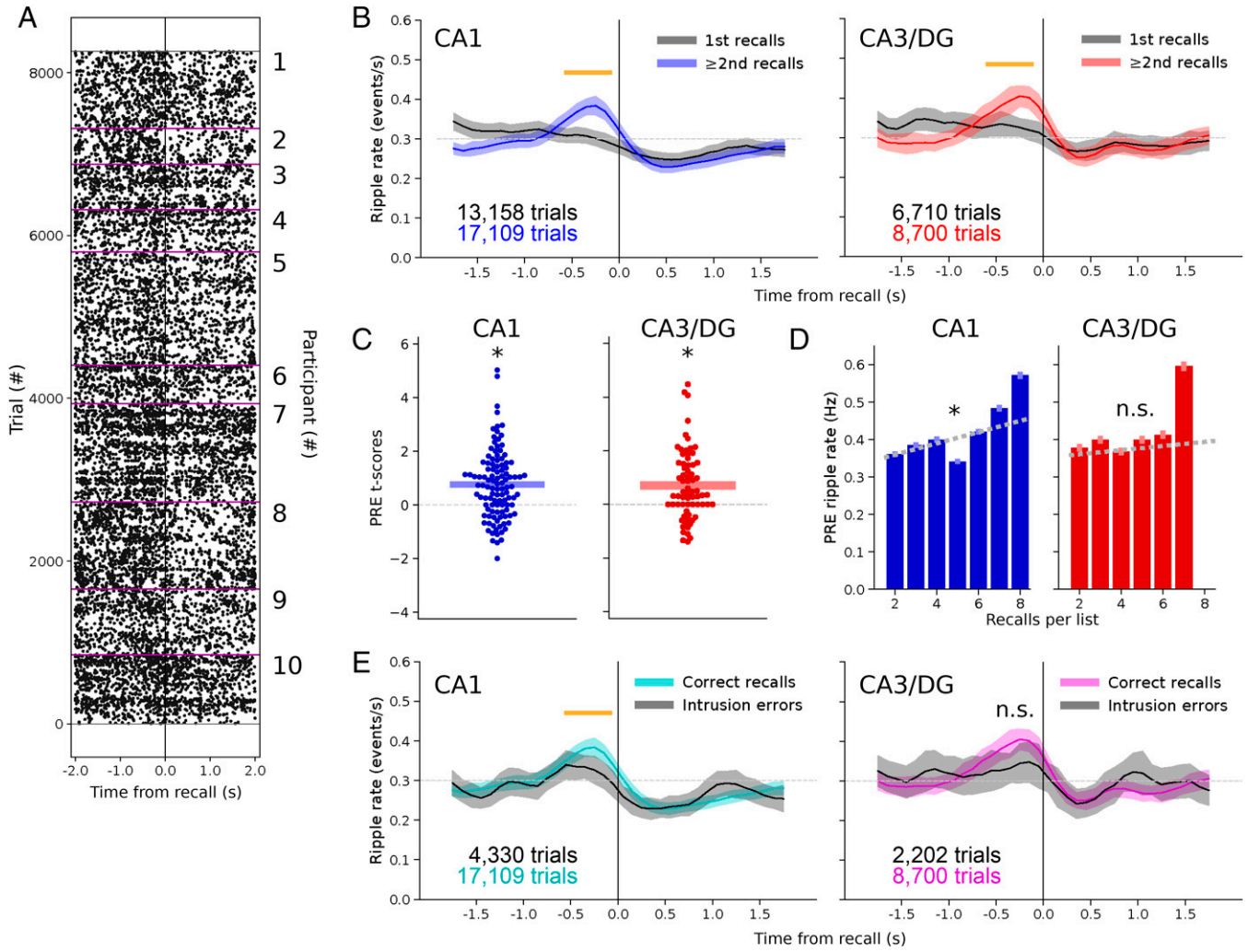

Fig. 2. High-frequency ripples increase in hippocampal subfields CA1 and DG shortly before free recall. (*A*) Raster plot aligned to free recall for all hippocampally localized electrode pairs in 10 selected participants. Each dot represents the start time of a ripple. Purple lines divide participants. (*B*) PVTHs for hippocampal subfields CA1 and CA3/DG separated by whether the recall was the first made during the retrieval period or ≥second during the retrieval period for the FR dataset. Trial numbers for each are labeled, where a trial is defined as a single recall on a single electrode pair. Significance of mixed model assessing the PRE for ≥second recalls (Eq. **1**): held-out data: CA1, $\beta = 0.073 \pm 0.019$, $P = 7.9 \times 10^{-4}$; CA3/DG, $\beta = 0.039 \pm 0.024$, $P = 0.20$; 100% of data: CA1, $\beta = 0.067 \pm 0.014$, $P = 2.1 \times 10^{-5}$; CA3/DG, $\beta = 0.049 \pm 0.018$, $P = 0.015$ (FDR-corrected across six tests of Eq. **1** across Figs. 2–4). CA1: 262 sessions from 130 participants. CA3/DG: 175 sessions from 84 participants. Error bands are SE from a separate mixed model calculated at each time bin. To aid visual comparison between PVTHs throughout the paper, a dotted gray line is added. The orange line indicates significant time range. (*C*) *t* scores for each participant from a mixed model assessing PRE for ≥second recalls by comparing the ripple rate from −600 to −100 ms before vocalization with the rate at −1,600 to −1,100 ms for areas CA1 and CA3/DG (Eq. **2**). Positive values indicate a stronger PRE. Participant count: CA1, $n = 110$; CA3/DG, $n = 69$ with at least 10 recalls. Bars indicate ±1 SE from mean. One-sample *t* test of *t* scores from Eq. **2** vs. 0: held-out data: CA1, $P = 1.2 \times 10^{-4}$, $t = 4.4$, df = 70; CA3/DG, $P = 1.6 \times 10^{-3}$, $t = 3.6$, df = 46; 100% of data: CA1, $P = 1.4 \times 10^{-7}$, $t = 6.1$, df = 109; CA3/DG, $P = 4.3 \times 10^{-5}$, $t = 4.6$, df = 68 (FDR-corrected for six *t* tests across Figs. 2–4). (*D*) Ripple rate during the PRE window for trials on a list vs. the number of recalls on that list. Bars are mean ± SE (light). Significance of the interaction between PRE ripple rate and number of recalls per list is assessed via a mixed model (Eq. **3**): CA1, $\beta = 0.013 \pm 0.004$, $P = 8.3 \times 10^{-4}$; CA3/DG, $\beta = 0.005 \pm 0.012$, $P = 0.64$ (FDR-corrected across two tests). Same participant *n* as *C*. (*E*) PVTHs for correct ≥second recalls vs. ≥second intrusions. Conventions and participant *n* are the same as *B*. Significance of PRE for correct vs. intrusion trials (Eq. **1**): held-out data: CA1, $\beta = 0.039 \pm 0.024$, $P = 0.22$; CA3/DG, $\beta = -0.006 \pm 0.040$, $P = 0.88$; 100% of data: CA1, $\beta = -0.042 \pm 0.018$, $P = 0.044$; CA3/DG, $\beta = -0.012 \pm 0.031$, $P = 0.70$ (FDR-corrected across two tests). $^*P < 0.05$. N.s., not significant.

a significantly stronger PRE in CA1 when they remember more list items (Fig. 2*D* and Eq. **2**). Another way to relate PRE with memory performance is to compare correct recalls with intrusions [i.e., recall of items not present on the target list (31)]. We find a significantly stronger PRE for correct recalls than intrusions in CA1 (Fig. 2*E*). Although trending in the same direction, these comparisons do not appear significantly in CA3/DG. Taken together, the link between PRE and correct, cue-dependent recall implicates hippocampal ripples in episodic memory retrieval.

PRE Is Stronger in Hippocampus than the ENT or PHC Cortex. In addition to hippocampal electrode pairs, many participants had electrode coverage in the ENT and PHC cortex (Fig. 3*A*). Ripples are known to occur in both of these regions (1, 15), so, once again using the FR dataset, we ask if PRE occurs in these regions before vocalization, as shown in the hippocampus. Neither the ENT or PHC cortex show a significant PRE when comparing ≥second recalls to first recalls when averaging recordings across all participants (Fig. 3*C* and Eq. **1**). When assessing PRE at the participant level as the rise in ripples before vocalization compared to baseline rates for ≥second recalls, the ENT cortex does not show a significant rise in ripples (Fig. 3*D* and Eq. **2**). However, PHC cortex does show a significant rise in ripples compared to baseline (Fig. 3*E* and Eq. **2**).

To properly compare PRE between regions, we contrast them in a single model for each participant. We make pairwise

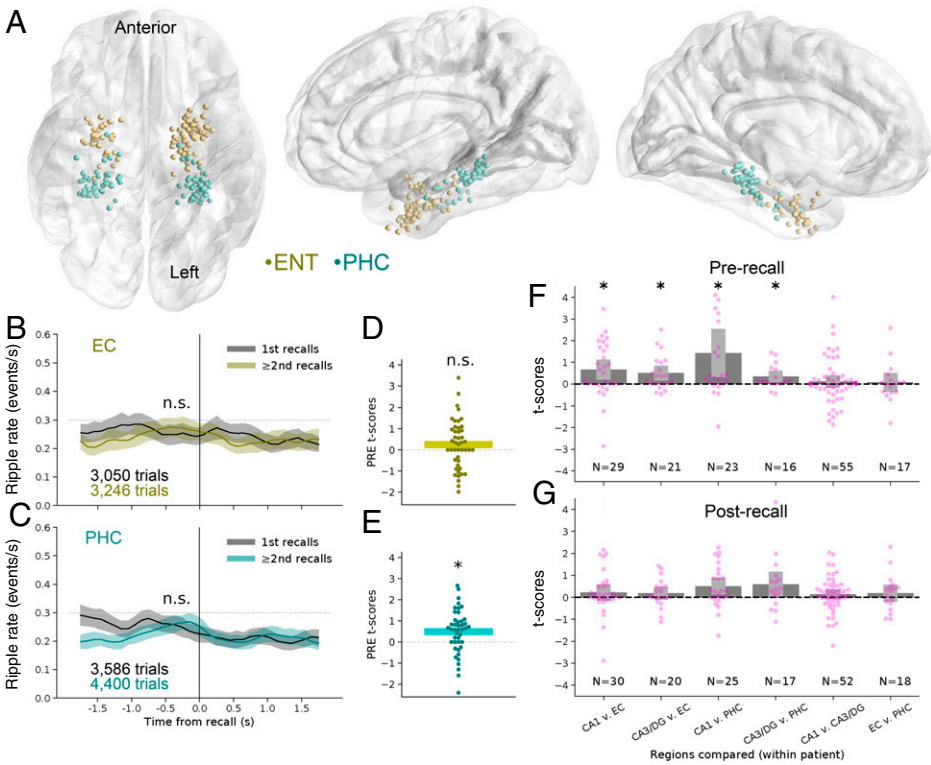

Fig. 3. Regional differences in the PRE. (*A*) Localization of extrahippocampal electrode pairs as in Fig. 1*E*. From left to right: ventral, left sagittal, and right sagittal. ENT, $n = 114$ bipolar electrode pairs; parahippocampal (PHC), $n = 128$. (*B*) PVTH for ENT cortex trials, separated by first recall and ≥second recalls from each list for FR dataset. Significance of mixed model assessing PRE for ≥second recalls (Eq. **1**): held-out data: $\beta = 0.041 \pm 0.033$, $P = 0.31$; 100% of data: $\beta = 0.029 \pm 0.024$, $P = 0.35$ (FDR-corrected across six tests of Eq. **1**). Data are from 113 sessions from 65 participants. Error bands are SE from a mixed model at each bin, and the orange line indicates significant time range as in Fig. 2. (*C*) Same for parahippocampal cortex. Held-out data: $\beta = 0.013 \pm 0.025$, $P = 0.59$; 100% of data: $\beta = 0.004 \pm 0.020$, $P = 0.86$. Data are from 117 sessions from 67 participants. (*D*) Same conventions as Fig. 2*C*, with mixed-model *t* scores of the rise in ripples over baseline for PRE calculated for ENT electrode pairs in each participant (Eq. **2**). Held-out data: $P = 0.27$, $t = 1.2$, df = 32; 100% of data: $P = 0.15$, $t = 1.5$, df = 44 (FDR-corrected across 6 tests). $n = 45$ participants. (*E*) Same for parahippocampal cortex. Held-out data: $P = 0.063$, $t = 2.1$, df = 29; 100% of data: $P = 0.0057$, $t = 3.1$, df = 42 (FDR-corrected across six tests). $n = 43$ participants. (*F*) Mixed-model *t* scores of pairwise comparisons of PRE for each participant with electrodes in at least two of the four regions under study: hippocampal areas CA1 and CA3/DG, as well as ENT cortex (EC) and parahippocampal cortex (PHC). The model assesses PRE for ≥second recalls from a time range −600 to −100 ms before vocalization (Eq. **4**). Asterisks indicate that the first of the pair being compared is significantly greater than the second. *$P < 0.05$ (FDR-corrected for six pairwise comparisons of prerecall ripples using Eq. **4**). N.s., not significant. Sample size of participants is indicated at the bottom of each comparison. Error bars are SE. (*G*) Similar to *F*, but for a mixed model assessing a drop in ≥second recalls from a time range 200 to 700 ms after vocalization between regions (Eq. **4**). No comparison shows a significant drop in ripples after recall ($P < 0.05$, FDR-corrected for six pairwise comparisons of postrecall ripples using Eq. **4**). Error bars are SE.

comparisons between the hippocampal subfields (CA1 and CA3/DG) and the ENT and PHC cortices, but only for those participants with bipolar electrode pairs in at least two of these regions (e.g., a participant with electrodes in CA1, CA3/DG, and the ENT cortex would contribute three pairwise comparisons: CA1 vs. CA3/DG, CA1 vs. ENT, and CA3/DG vs. ENT). Comparing PRE between pairs of regions within each participant using a separate linear mixed model for each (Eq. **4**) isolates the region contrast by controlling for differences between participants (i.e., recordings from both regions occur during the same recalls). The *t* scores from each model are then combined across regional comparisons and assessed with a one-sample *t* test across participants (Fig. 3*F*). Both hippocampal subfields CA1 and CA3/DG have a significantly stronger PRE than the ENT or PHC cortex. There are no reliable differences in PRE between CA1 and CA3/DG or between the ENT and PHC cortex. We also ask whether the postvocalization drop in ripple rate evident in many participants (Fig. 2 *A* and *B*), possibly due to a refractory period after the rise in ripples from PRE (1, 32), is also specific to the hippocampus. Taking advantage of these same participants with electrode pairs in at least two regions, no pair of regions show a significant difference after vocalization (Fig. 3*G* and Eq. **4**), suggesting that this drop is not specific to the hippocampus like PRE. In conclusion, PRE predominantly occurs in the hippocampus.

PRE Is Stronger for Contextually Mediated Recalls. Next, we ask if PRE correlates with behavioral measures specific to episodic memory (31, 33, 34). We first focus on the catFR dataset, as the list of words in this task has a rich semantic and temporal structure (Fig. 4*A*). In particular, words in the catFR task are drawn from a pool of 25 semantically related categories, with 3 categories selected per 12-word list. Each set of 4 words from a category is presented as pairs, with the pairs never shown back-to-back. For example, "dolphin" and "octopus" might be a pair of consecutively shown words, followed by "cupcake" and "pie," which are then followed by "fish" and "whale" (Fig. 4*A*). This setup allows us to measure contextual reinstatement in semantic and temporal dimensions when participants recall the words, as back-to-back recalls can transition between 1) a semantic pair that was temporally adjacent in the list (adjacent semantic, e.g., "dolphin…octopus"; 20% of recalls); 2) a semantic pair that was temporally remote in the list (remote semantic, e.g., "dolphin…whale"; 20% of recalls); and 3) a pair of words that were temporally adjacent in the list, but not semantically related (only 3% of recalls, as participants tend to recall via semantic associations in catFR, so we do not investigate them further). The remaining transitions are remote unclustered (e.g., "dolphin…pie"; 17% of recalls), meaning two semantically unrelated words that were not adjacent on the list; intrusions (12%); and dead ends (28%). By comparing groups of trials with contextual associations to those without, we can assess if ripples

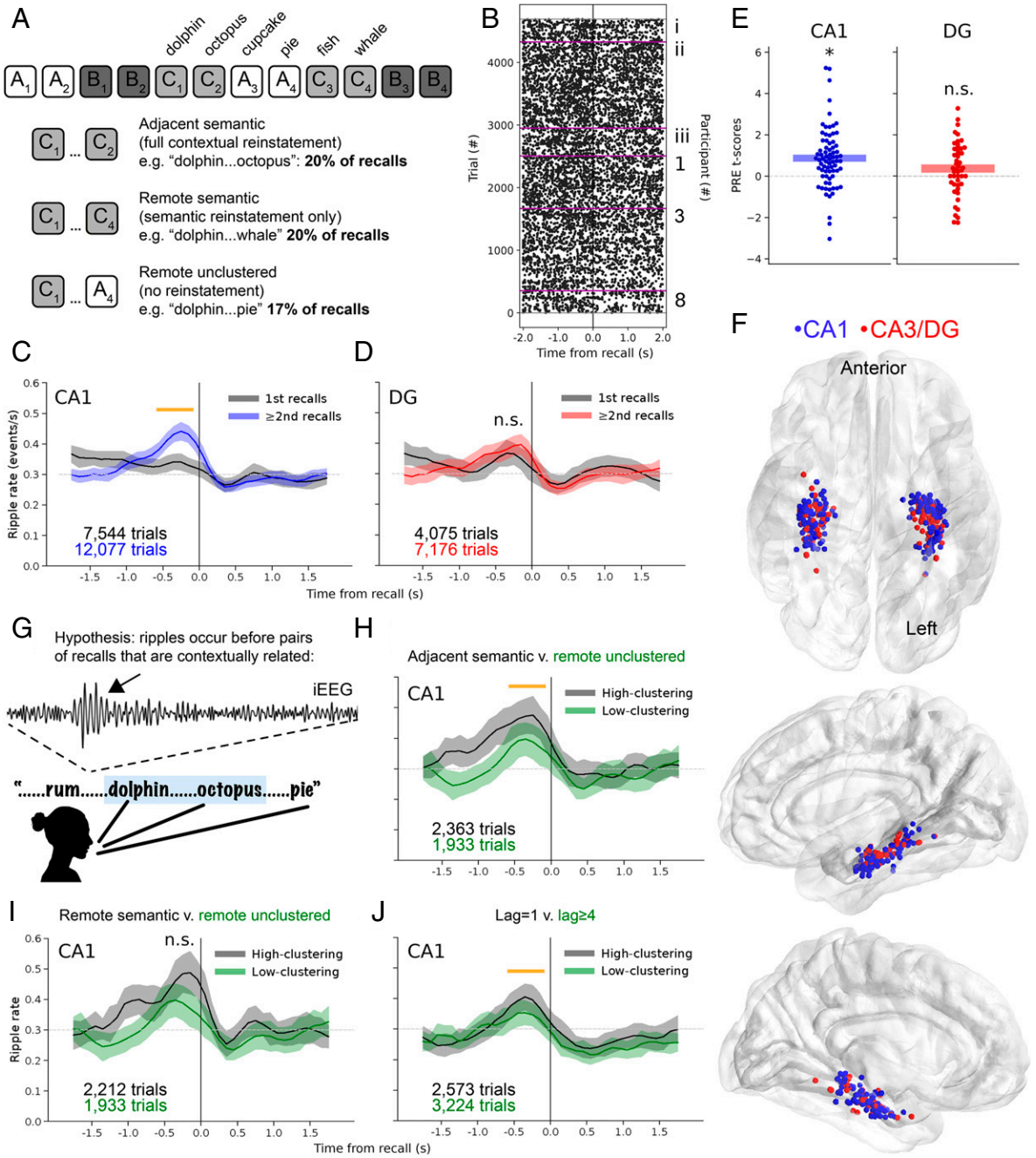

Fig. 4. Context reinstatement and the PRE. (*A*, *Upper*) Outline of categorized free recall task (catFR). Word lists comprised 12 words from 3 semantic categories (shown as A_x, B_x, and C_x) and are presented during encoding in pairs of 2. (*A*, *Lower*) Percentages of recall types by transitions between recalls. (*B*) Raster of ripples aligned to vocalization from three of the same participants in Fig. 2*A* that ran both task versions (1, 3, and 8) and three new participants (I through iii). Purple lines divide participants. (*C*) PVTH for hippocampal subfield CA1 aligned to vocalization in catFR with the same conventions as Fig. 2*B*. Significance of mixed model assessing PRE for ≥second recalls (Eq. **1**): held-out data: $\beta = 0.065 \pm 0.025$, $P = 0.033$; 100% of data: $\beta = 0.077 \pm 0.019$, $P = 2.2 \times 10^{-4}$ (FDR-corrected across six tests of Eq. **1**). There were 163 sessions from 89 participants. Error bands are SEs from a mixed model at each bin, and the orange line indicates significant time range, as in Figs. 2 and 3. (*D*) Same for hippocampal area CA3/DG. Held-out data: $\beta = 0.029 \pm 0.032$, $P = 0.44$; 100% of data: $\beta = 0.023 \pm 0.025$, $P = 0.42$. Data are from 115 sessions from 61 participants. (*E*) Same conventions as Fig. 2*C*, with mixed-model *t* scores for PRE calculated for CA1 and CA3/DG electrode pairs in each participant performing catFR (Eq. **2**). Held-out data: CA1, $P = 1.2 \times 10^{-4}$, $t = 4.6$, df = 48; CA3/DG, $P = 0.32$, $t = 1.0$, df = 28; 100% of data: CA1, $P = 6.7 \times 10^{-6}$, $t = 5.1$, df = 73; CA3/DG, $P = 0.064$, $t = 2.0$, df = 47 (FDR-corrected across six tests). CA1, $n = 74$; CA3/DG, $n = 46$ with at least 10 recalls. (*F*) Localization of hippocampal electrode pairs in participants that ran catFR, as in Fig. 1*E*. Views from top to bottom are inferior, left sagittal, and right sagittal. CA1, $n = 219$ bipolar electrode pairs; CA3/DG, $n = 122$. (*G*) Schematic for hypothesis of ripples as a signature of contextual reinstatement. An example ripple before vocalization is shown (arrow) in zoomed-in iEEG (70 to 178 Hz filtered). (*H*) PVTH of catFR trials comparing adjacent semantic vs. remote unclustered trials, aligned to the first word of each pair. Significance of coefficient comparing PRE between these trial types in a mixed model (Eq. **1**): held-out data: CA1, $\beta = -0.074 \pm 0.049$, $P = 0.20$; 100% of data: CA1, $\beta = -0.089 \pm 0.036$, $P = 0.046$ (FDR-corrected across six tests of Eq. **1**; Fig. 4 *H–J* and *SI Appendix*, Fig. S3 *A–C*). We also compare using the same model with the PRE window from −1,100 to −100 ms: 100% of data: CA1, $\beta = -0.077 \pm 0.024$, $P = 0.0080$ (FDR-corrected across six tests using this window). Data are from 145 sessions collected in 83 participants. Error bands are SE, and the orange line indicates significant time range. (*I*) PVTH of catFR trials comparing remote semantic vs. remote unclustered trials. Same conventions, number of sessions and participants, and significance test as *H*. Held-out data: CA1, $\beta = -0.024 \pm 0.051$, $P = 0.64$; 100% of data: CA1, $\beta = -0.053 \pm 0.051$, $P = 0.20$ (FDR-corrected). Using the bin from −1,100 to −100 ms: 100% of data: CA1, $\beta = -0.066 \pm 0.025$, $P = 0.027$ (FDR-corrected). (*J*) PVTH of FR data comparing adjacent recalls (lag = 1) vs. remote recalls (lag ≥ 4). Data are from 199 sessions collected in 109 participants. Same conventions and significance test as *H*. Held-out data: CA1, $\beta = -0.075 \pm 0.036$, $P = 0.11$; 100% of data: CA1, $\beta = -0.061 \pm 0.036$, $P = 0.035$ (FDR-corrected). Using the bin from −1,100 to −100 ms: 100% of data: CA1, $\beta = -0.029 \pm 0.024$, $P = 0.22$ (FDR-corrected). *$P < 0.05$. N.s., not significant.

not only precede recall, but preferentially precede reinstatement of contextual information used to remember groups of items with related features, a key signature of episodic memory (18). Note that we only use ≥second recalls in these analyses, as the first recall in every list does not show the signature PRE (Figs. 2*B* and 4 *C* and *D*), possibly due to weaker contextual reinstatement before the first recall (*Discussion*).

Before assessing differences between types of recall, we confirm that our main findings hold true in the catFR dataset, which also acts as an independent dataset to test the presence of PRE. First, using three of the same participants that contributed to the FR raster plot and three new participants (Fig. 2*A*), a raster aligned to vocalization for the catFR task once again shows visual evidence of PRE (Fig. 4*B*). Across all participants, PRE is significant for ≥second recalls compared to first recalls in both CA1 (Fig. 4*C*) and CA3/DG (Fig. 4*D*). Looking at participants individually, there is a significant rise in ripples above baseline for ≥second recalls across participants in CA1 and in the same direction for CA3/DG (Fig. 4*E*). However, due to randomness in participant electrode montages, there happened to be many fewer electrode pairs in CA3/DG than CA1 for catFR (132 vs. 241, respectively; Fig. 4*F*), making tests with this subfield for catFR relatively underpowered.

For the first test of contextual reinstatement, we set up a comparison between those recalls that act as the strongest contextual cues compared to those that act as the weakest. In particular, we contrast adjacent semantic trials (Fig. 4*A*), where the subsequent recall was both temporally adjacent and semantically related to the previous recall on the list; and remote unclustered trials, where the subsequent recall was neither. The hypothesis is that if ripples are a signature of contextual reinstatement, we expect PRE before vocalization of the related pair of words (Fig. 4*G*). For example, if a participant recalls "dolphin…octopus," the expectation is that PRE will occur before "dolphin," as the reinstatement of context that leads to "octopus" occurs before either word is vocalized (20, 35). We do not expect such a signature of reinstatement to occur before unclustered words (e.g., "dolphin…pie"). Indeed, in CA1, when aligning the PVTH to the first word of adjacent semantic pairs, PRE is significantly stronger than when aligning the PVTH to the first word of remote unclustered pairs (Fig. 4*H*). CA3/DG does not show a significantly greater PRE for adjacent semantic trials for this comparison (*SI Appendix*, Fig. 3*A*).

For the second test of contextual reinstatement, we compare remote semantic and remote unclustered recalls (Fig. 4*A*). This comparison isolates semantically driven transitions, as these same-category recalled pairs did not appear in adjacent list positions. PRE does not meet our significance threshold when aligning to the first word in remote semantic trials for CA1 (Fig. 4*I*). However, when assessing PRE from −1,100 to −100 ms instead of the typical −600 to −100 ms, which more clearly matches the separation between the two curves after incorporating data from the held-out data, a significant difference exists between these trials in CA1 (Fig. 4*I*). There is no significant difference for these groups in CA3/DG (*SI Appendix*, Fig. 3*B*).

For the third test of contextual reinstatement, we aim to isolate temporal clustering based on the presentation order of the word list. Since the catFR task is designed to promote semantic associations, we return to the FR task, where the 12 words are not designed to be semantically related (Fig. 1*A*). To assess temporal clustering, we group all recalls that lead to adjacent transitions from the list (absolute lag = 1, e.g., "chalk…bat"; 16% of transitions) and compare them to all recalls that led to remote transitions on the list (absolute lag ≥ 4; 20%) (36). The hypothesis remains the same: that when we align the PVTH to the first word of the recalled lag = 1 pair, PRE should signal reinstatement prior to the vocalization of the pair of recalls, but not when we align to lag ≥ 4 pairs. For CA1, recalls that lead to such temporally clustered transitions show a stronger PRE than recalls that lead to remote transitions (Fig. 4*J*). CA3/DG also shows a significant difference in PRE between lag = 1 and lag ≥ 4 pairs, although only when assessing PRE from −1,100 to −100 ms instead of −600 to −100 ms (*SI Appendix*, Fig. 3*C*).

For each of these three tests of contextual reinstatement, we hypothesize that PRE occurs prior to the vocalization of the pair of related words. For example, if the words "dolphin" and "octopus" are presented back-to-back during encoding and the participant subsequently recalls these two words consecutively (as in Fig. 4*G*), for this adjacent semantic transition, we expect a rise in ripples prior to vocalization of the word "dolphin." An alternative possibility is that the person recalls "dolphin," the item-to-context reinstatement (25) takes time to occur, and the subsequent context-to-item process produces the word "octopus" only after the vocalization of "dolphin." In this case, we would expect to see a rise in ripples prior to "octopus" (i.e., before the second word in the transition). Instead, we see an "anti-PRE effect": CA1 ripple rates are lower prior to the second word in adjacent semantic and remote semantic pairs for catFR, and lower prior to the second word in lag = 1 pairs for FR (*SI Appendix*, Fig. 4), as compared to the low-clustering conditions in each case. These results suggest that ripples mark item-to-context reinstatement, as we expand on in *Discussion*.

Hippocampal PRE Is Not an Artifact of Localization, Detection Algorithm, or Epilepsy. The localization of each bipolar electrode pair to the CA1 or CA3/DG hippocampal subfields is taken as the midpoint between adjacent electrode contacts (electrode spacing is between 3 and 10 mm; *Materials and Methods*). However, if either of the two contacts are outside the subfield, the ripples for a pair could possibly originate from a different region. To prove that ripples indeed originate from both CA1 and CA3/DG, we perform a control analysis using only the CA1 pairs where both contacts were individually localized to CA1 or only the CA3/DG pairs where both contacts were individually localized to CA3/DG (*SI Appendix*, Figs. 5 and 6). Even with these more conservatively selected pairs that reduce the trial count by more than half, we find a statistically significant PRE in CA1 (*SI Appendix*, Figs. 5 and 6). Although the PRE in CA3/DG shows similar ripple rates, it does not meet our statistical threshold, likely owing to the substantial reduction in trials.

The frequency range for the ripple-detection algorithm—based on a recent study of human hippocampal ripples (11)—is relatively broad (70 to 178 Hz). This range likely includes sharp-wave ripple-associated fast gamma, as well as ripples (37, 38). Whereas previous work has grouped these events, as they differ only in frequency and relative amplitudes between subfields (37, 38), we ask if ripples detected using algorithms with narrower ranges still reliably show PRE. For a first check, we implement a ripple-detection algorithm with a narrower range (80 to 120 Hz) that was recently used to identify ripples in MTL (12, 15, 16). This stricter algorithm yields lower ripple rates, and ripples have a peak ripple frequency of ∼90 Hz (*SI Appendix*, Figs. 1*C* and 7*A*), as in previous work (12, 15, 16). Despite the lower ripple rates, we find a significant PRE for ≥second recalls compared to first recalls in CA1 and in the same direction for CA3/DG (*SI Appendix*, Fig. 7*B*). For a second check, we utilize the original ripple-detection algorithm, but with a higher frequency range (125 to 200 Hz) to isolate ripples at frequencies typically reported in rodent sharp-wave ripple work (1, 37). This method yields lower ripple rates, has a shorter

distribution of durations than the original algorithm, and yields a frequency peak of ∼150 Hz (*SI Appendix*, Figs. 1*B* and 8*A*). We do not find a significant PRE for ≥second recalls compared to first recalls in CA1 or CA3/DG using this algorithm (*SI Appendix*, Fig. 8*B* and Eq. **1**), owing to the false discovery rate (FDR) correction, although there is a significant rise in ripples for CA1 compared to baseline rates (*SI Appendix*, Fig. 8*B* and Eq. **2**).

We also address the possibility that PRE relates to seizurogenic tissue in epileptic participants, even though recent work suggests that epileptiform tissue shows a weaker link between ripples and memory than healthy tissue (12). For those participants with a clinically defined seizure-onset zone (SOZ), we take all trials from bipolar pairs in the SOZ and compare them to all trials from bipolar pairs not in the SOZ. For both the CA1 and CA3/DG groups, SOZ and non-SOZ trials show a significant PRE (*SI Appendix*, Fig. 9*A*). However, neither subfield shows a significant difference when comparing PRE between them, dissociating PRE from epileptic activity. In sum, these control analyses suggest that PRE occurs regardless of detection methods and seizure activity.

Discussion

We investigate high-frequency ripples as participants study and subsequently recall lists of unrelated items ($n = 195$) or lists of categorically related items ($n = 126$). In both paradigms, we find a punctate rise in ripples immediately before participants say recalled words. This prerecall retrieval effect (PRE) occurs specifically for recalls that follow previously recalled items, thereby signaling a cue-dependent retrieval process (Figs. 2*B* and 4 *C* and *D*). In particular, we find the highest ripple rates for PRE prior to contextually reinstated recalls (Fig. 4 *H–J*). PRE also appears more significantly in hippocampal subfields CA1 and CA3/DG compared to the ENT and PHC cortex (Fig. 3*G*). These results implicate ripples in hippocampally-initiated episodic memory retrieval.

The free-recall task provides a window into the organization of memory because it permits participants to report studied items in the order that they come to mind. The order and timing of recalled items reveals the temporal and semantic organization of memory, as participants tend to consecutively recall temporally proximate or semantically related items (39). Modeling these dynamics of memory search highlights the importance of context: a latent representation that includes information about time, space, and semantics of recently experienced or recalled items (25). According to these models, retrieving an item from memory brings about its prior contexts, which, in turn, triggers the next item that comes to mind. Meanwhile, persistent context from the end of the list governs the first recall from each list, as there is no preceding item to cue context retrieval (30, 40). Here, we find a stark dichotomy between the first recall on each list and subsequent recalls, with PRE specifically occurring before subsequent recalls (Figs. 2*B* and 4 *C* and *D*), suggesting that hippocampal ripples represent a physiological correlate for retrieved context.

The clustering results further ballast the link between hippocampal ripples and contextual reinstatement, as recalls with strong semantic and/or temporal association to the next recalled word show significantly stronger PRE compared to recalls with low clustering (Fig. 4 *H–J*). Standard context-based theories (25) assert that retrieval of an item's perceptual-semantic features (e.g., those of "dolphin"; Fig. 4*G*) should precede the reinstatement of the item's associated context features (e.g., sea-animal category). Simultaneously with this item-to-context process, these models assume a dynamic decision-making process (41) that will eventually lead to item vocalization. We hypothesize that context reinstatement precedes this first vocal response and that PRE signals the process. Consistent with this theory, aligning to the vocalization of the subsequently recalled item (e.g., "octopus" in Fig. 4*G*) exhibits an anti-PRE (*SI Appendix*, Fig. 4), suggesting that context has already been reinstated prior to the first word. Context-based theories further predict that memory search evolves by using the reinstated context to guide retrieval of the next item (25). This context-to-item process necessarily would happen after context reinstatement and, therefore, have a later latency. One could thus interpret our findings as consistent with the idea that PRE reflects item-to-context retrieval and inconsistent with the idea that PRE reflects context-to-item retrieval. In this case, the apparent buildup in ripples prior to recall actually reflects a distribution of decision times from a stochastic drift-diffusion process (18, 41). Future work could pursue model-based analyses to elucidate the dynamics of PRE as it relates to the timing of sequentially recalled items.

The rate of ripples in human hippocampus might appear low for a marker of contextually mediated recall, with peak rates only reaching ∼0.5 Hz during the strongest conditions for reinstatement (Fig. 4 *H–J*). However, several aspects of depth electrode recordings place an upper bound on the measured ripple rates in our study. First, taking the spatial spread of the macroelectrode local field potential (LFP) as a radius of 1.5 mm (42) and the density of neurons in the human hippocampus to be 25,000 to 100,000/mm^3 (43, 44), an estimated 350,000 to 1,500,000 hippocampal neurons contribute to the LFP. Considering that the hippocampus contains ∼20,000,000 neurons in gray matter (43), a bipolar pair of electrodes might only sample from ∼1/7th to 1/30th of the hippocampus. Indeed, in the rodent hippocampus, most ripples are spatially confined to a few millimeters (45). Consequently, detecting ripples might not be common on many trials, even in the case that a participant has multiple probes in the region. Second, several factors, such as poor proximity to ripple-generating circuits (1), signal quality, and gliosis, can all conspire to reducing ripple detection. Third, some recalls may not rely on hippocampally mediated episodic memory processes (46). Fourth, ripple rates shown here exceed those reported in previous nonhuman primate (6, 7) and human work (15), although this depends on detector settings, as shown in *SI Appendix*, Figs. 7 and 8.

Recordings from hippocampal subfield CA1 represent the best evidence for ripples signaling contextually mediated reinstatement, as PRE is robust across the FR (Figs. 2, 3, and 4*J*) and catFR (Fig. 4 *A–I*) datasets. While the results are not as clear for the CA3/DG subfields, we present the same analyses because 1) CA3/DG is the only other hippocampal subfield where a large number of contacts were localized; and 2) CA3/DG shows significantly stronger PRE than ENT or PHC cortices (Fig. 3*F*). Not many of the CA3/DG contacts were likely to physically be in DG due to its relatively small volume (43), although because DG has significantly more neurons compared to other subfields, LFP from this group likely reflects combined activity across DG and neighboring CA2, CA3, and CA4. Future work using more precise localization could distinguish the origin of CA3/DG PRE and determine if the distinction found in rodents between fast gamma—as found in DG (37)—and ripples—expected in CA2/CA3—holds true for primates and maps onto specific behaviors.

In sum, hippocampal ripples preferentially occur before those recalls most likely to be achieved via contextual reinstatement of episodic memories. Our results support the hypothesis—developed from decades of rodent work—that ripples mediate episodic memory retrieval (10). While prior studies have linked high-frequency oscillations to memory retrieval in

humans (47, 48), using methods developed to isolate ripples, we uncover a clear physiological distinction between hippocampal and MTL cortical regions during episodic retrieval. Considering that episodic memory models implicate an inability to reinstate context in amnesics with MTL damage (21), these results suggest a link between memory loss and ripple malfunction.

Equations

Linear mixed-effects models are run by using the function MixedLM in the python package statsmodels with restricted maximum likelihood and Nelder–Mead optimization with a maximum of 2,000 iterations. The following equations are written in pseudocode of the inputs to statsmodels. Statistics are presented as: $\beta \pm \text{SE}$, P value, where β is the coefficient being tested in Eqs. **1**–**4**.

To compare PRE between two groups of trials—i.e., first vs. ≥second recalls (Figs. 2*B*, 3 *B* and *C*, and 4 *C* and *D*), high- vs. low-clustering trials (Fig. 4 *H–J*), correct vs. intrusion trials (Fig. 2*E*), or SOZ vs. non-SOZ (*SI Appendix*, Fig. 9)—we use the linear mixed-effects model:

$$\begin{aligned} ripple\_rate \sim\ & group\_indicator \\ & + (group\_indicator|participant) \\ & + (group\_indicator|participant:session), \end{aligned} \quad \textbf{[1]}$$

where $group\_indicator$ is zero for the first group of trials and one for the second group of trials, $(group\_indicator|participant)$ is a random intercept and slope for each participant, $(group\_indicator|participant:session)$ is a random intercept and slope for each session nested in participants, and $ripple\_rate$ is the ripple rate in the bin from −600 to −100 ms aligned to vocalization (unless otherwise stated). The null hypothesis is no difference in PRE between the two groups. Negative coefficients indicate a decrease in ripples between the first and second group (e.g., a drop from ≥second to first recalls).

We also investigate PRE individually for each participant (Fig. 2*C*). We fit a linear mixed model on the participant's ≥second recall trials:

$$ripple\_rate \sim bin\_indicator + (1|session), \quad \textbf{[2]}$$

where $bin\_indicator$ is zero for the bin −1,600 to −1,100 ms and one for the bin −600 to −100 ms aligned to time of vocalization; $1|session$ is a random intercept for different sessions; and the other factors are the same as in Eq. **1**. The null hypothesis is no difference in ripple rate between the −600- to −100-ms bin and the same bin aligned 1 s earlier. We note that using the comparison between the PRE bin and the bin 1 s earlier is effectively a different test of PRE than using first vs. ≥second recalls, as in Eq. **1**. Therefore, Eqs. **1** and **2** show that PRE is both stronger for ≥second recalls and rises above the basal ripple rates prior to recall, respectively.

To test the hypothesis that participants with better memories show a stronger PRE (reported in the legend of Fig. 2*D*), we used the linear mixed-effects model:

$$\begin{aligned} ripple\_rate \sim\ & num\_recalls + (num\_recalls|participant) \\ & + (num\_recalls|participant:session), \end{aligned} \quad \textbf{[3]}$$

where $num\_recalls$ is the number of total recalls by the participant from the list the trial came from, $ripple\_rate$ is the rate in the bin −600 to −100 ms, and the other factors are random effects for participant and session nested in participant, as in Eq. **1**. The null hypothesis is no difference between number of recalls per list and change in ripple rate.

To make pairwise comparisons between regions to test if some regions have a stronger PRE than others (Fig. 3*G*), we used the linear mixed-effects model:

$$\begin{aligned} ripple\_rate \sim\ & region\_indicator \\ & + (region\_indicator|session), \end{aligned} \quad \textbf{[4]}$$

where $region\_indicator$ is zero or one for two different regions (in the order shown beneath each swarm plot in Fig. 3*G*), $(region\_indicator|session)$ is a random intercept and slope for each session, and $ripple\_rate$ is the ripple rate in the bin from −600 to −100 ms aligned to vocalization. Note that every test is for bipolar electrode pairs in different regions for the same participant; therefore, only variance across sessions had to be accounted for. The null hypothesis is no difference in PRE between regions. Significance for each of the six pairwise comparisons is assessed with an FDR-corrected (Benjamini–Hochberg) t test to correct for the six comparisons.

We also made pairwise comparisons between regions for postrecall ripples (Fig. 3*H*). The equation is the same as Eq. **4**, except that the ripple rates are from the bin 200 to 700 ms after recall.

Materials and Methods

Detailed methods are provided in *SI Appendix*.

Human Participants. The dataset includes 245 adult participants in the hospital for medication-resistant epilepsy with subdural electrodes placed on the cortical surface or within the brain for the purpose of localizing epileptic activity (49). All participants gave their informed consent to participate in this research study. Data were recorded at eight hospitals from 2015 to 2021. The research protocol and informed-consent process were approved by the Institutional Review Board (IRB) at the University of Pennsylvania. Each participating hospital was sanctioned for research under a reliance agreement with the University of Pennsylvania IRB.

Tasks. Participants performed two versions of delayed free-recall tasks, where they viewed lists of words and subsequently recalled as many words as they could. Each list consisted of four phases: countdown, encoding, distractor, and retrieval. After a 10-s countdown, the encoding period consisted of 12 words presented sequentially on a computer screen. After a math distractor, participants were tasked to vocalize as many words as they could remember during the retrieval period. The first version of the task (FR) used lists of words that were uncategorized. The second version of the task (catFR) used lists of words drawn from three semantic categories per list that were presented sequentially in pairs of two.

Recordings and Ripple Detection. iEEGs were recorded from subdural grids and strips (intercontact spacing 10.0 mm) or depth electrodes (intercontact spacing 3 to 10 mm) and referenced by using neighboring bipolar electrode pairs. We used an algorithm recently shown to isolate ripples in human hippocampus (11) that is based on sharp-wave ripple detection in rodents (38) and interictal epileptiform discharge removal in epileptic participants (50). Control algorithms used this same algorithm with a higher frequency range (125 to 200 Hz) and a second algorithm recently used to detect ripples in MTL (15). Ripples were treated as discrete events throughout the paper.

Anatomical Localization. Structural MRI and computed tomography scans were coregistered by using Advanced Normalization Tools (28) to align the brain regions to the electrode montage. The point source of iEEG for bipolar electrode pairs is considered to be the midpoint between adjacent electrode contacts. Bipolar pairs in hippocampal subfields CA1 and CA3/DG were localized by using a combination of neuroradiologist labels (Joel M. Stein and Sandhitsu Das, Penn Medicine, Philadelphia) and the automated segmentation of hippocampal subfields technique.

Plots. Recalls within 2 s of a previous recall were removed from consideration in order to avoid double-counting ripples. Therefore, every ripple in the raster and

PVTHs is a unique event. PVTHs were formed by binning ripples (100-ms bins) and averaging the raster plots across participants. For visualization only, PVTHs were triangle-smoothed by using a five-bin window (11), and a separate linear mixed model with sessions nested in participants was run at each bin to calculate the error bars (SE).

Held-Out Data and Preregistration. Due to the unparalleled size of our datasets [the FR dataset alone has 20x more trials than previous studies of ripples in humans (11, 12, 15)], we came up with initial hypotheses based on analysis of only ∼40% of the FR and catFR datasets. We registered these hypotheses on the Open Science Framework (https://osf.io/y5zwt). For each of these preregistered analyses, we present statistics for the held-out dataset. We also present statistics for the whole dataset for all analyses. Plots are shown using the whole datasets, and significance on figures is assessed using the whole datasets.

Data, Materials, and Software Availability. Data were collected as part of the Defense Advanced Research Projects Agency (DARPA) Restoring Active Memory (RAM) initiative and are available to the public (https://memory.psych.upenn.edu/Electrophysiological_Data). Code and processed data for all plots and analyses are available (https://memory.psych.upenn.edu/files/pubs/SakoKaha21.code.tgz) (49). We preregistered our hypotheses as well as the initial figures for the first half of the data on the Open Science Framework (https://osf.io/y5zwt)(51). Questions should be addressed to sakon@upenn.edu.

ACKNOWLEDGMENTS. Data were collected as part of the DARPA RAM program (Cooperative Agreement N66001-14-2-4032). This work is supported by NIH Grant R01NS106611-02 and US Army Medical Research and Development Command Medical Technology Enterprise Consortium Grant MTEC-20-06-MOM-013. The views, opinions, and/or findings contained in this material are those of the authors and should not be interpreted as representing the official views or policies of the Department of Defense or the US Government. We also thank the M.J.K. lab, the Joshua Jacobs lab, the György Buzsáki lab, the Anli Liu lab, the Ehren Newman lab, Alice Healy, Dan Levenstein, and Sam McKenzie for providing valuable feedback on this work.

1. G. Buzsáki, Hippocampal sharp wave-ripple: A cognitive biomarker for episodic memory and planning. *Hippocampus* **25**, 1073–1188 (2015).
2. N. K. Logothetis *et al.*, Hippocampal-cortical interaction during periods of subcortical silence. *Nature* **491**, 547–553 (2012).
3. W. E. Skaggs *et al.*, EEG sharp waves and sparse ensemble unit activity in the macaque hippocampus. *J. Neurophysiol.* **98**, 898–910 (2007).
4. K. Mizuseki, G. Buzsáki, Preconfigured, skewed distribution of firing rates in the hippocampus and entorhinal cortex. *Cell Rep.* **4**, 1010–1021 (2013).
5. W. Tang, S. P. Jadhav, Sharp-wave ripples as a signature of hippocampal-prefrontal reactivation for memory during sleep and waking states. *Neurobiol. Learn. Mem.* **160**, 11–20 (2019).
6. T. K. Leonard *et al.*, Sharp wave ripples during visual exploration in the primate hippocampus. *J. Neurosci.* **35**, 14771–14782 (2015).
7. T. K. Leonard, K. L. Hoffman, Sharp-wave ripples in primates are enhanced near remembered visual objects. *Curr. Biol.* **27**, 257–262 (2017).
8. A. Fernández-Ruiz *et al.*, Long-duration hippocampal sharp wave ripples improve memory. *Science* **364**, 1082–1086 (2019).
9. S. P. Jadhav, C. Kemere, P. W. German, L. M. Frank, Awake hippocampal sharp-wave ripples support spatial memory. *Science* **336**, 1454–1458 (2012).
10. H. R. Joo, L. M. Frank, The hippocampal sharp wave-ripple in memory retrieval for immediate use and consolidation. *Nat. Rev. Neurosci.* **19**, 744–757 (2018).
11. Y. Norman *et al.*, Hippocampal sharp-wave ripples linked to visual episodic recollection in humans. *Science* **365**, eaax1030 (2019).
12. S. Henin *et al.*, Spatiotemporal dynamics between interictal epileptiform discharges and ripples during associative memory processing. *Brain* **144**, 1590–1602 (2021).
13. Y. Y. Chen *et al.*, Stability of ripple events during task engagement in human hippocampus. *Cell Reports* **35**, 109304 (2021).
14. Y. Norman, O. Raccah, S. Liu, J. Parvizi, R. Malach, Hippocampal ripples and their coordinated dialogue with the default mode network during recent and remote recollection. *Neuron* **109**, 2767–2780.e5 (2021).
15. A. P. Vaz, S. K. Inati, N. Brunel, K. A. Zaghloul, Coupled ripple oscillations between the medial temporal lobe and neocortex retrieve human memory. *Science* **363**, 975–978 (2019).
16. A. P. Vaz, J. H. Wittig, Jr, S. K. Inati, K. A. Zaghloul, Replay of cortical spiking sequences during human memory retrieval. *Science* **367**, 1131–1134 (2020).
17. M. W. Howard, I. V. Viskontas, K. H. Shankar, I. Fried, Ensembles of human MTL neurons "jump back in time" in response to a repeated stimulus. *Hippocampus* **22**, 1833–1847 (2012).
18. S. M. Polyn, K. A. Norman, M. J. Kahana, A context maintenance and retrieval model of organizational processes in free recall. *Psychol. Rev.* **116**, 129–156 (2009).
19. J. R. Manning, S. M. Polyn, G. H. Baltuch, B. Litt, M. J. Kahana, Oscillatory patterns in temporal lobe reveal context reinstatement during memory search. *Proc. Natl. Acad. Sci. U.S.A.* **108**, 12893–12897 (2011).
20. E. A. Solomon, B. C. Lega, M. R. Sperling, M. J. Kahana, Hippocampal theta codes for distances in semantic and temporal spaces. *Proc. Natl. Acad. Sci. U.S.A.* **116**, 24343–24352 (2019).
21. D. J. Palombo, J. M. Di Lascio, M. W. Howard, M. Verfaellie, Medial temporal lobe amnesia is associated with a deficit in recovering temporal context. *J. Cogn. Neurosci.* **31**, 236–248 (2019).
22. H. R. Dimsdale-Zucker, M. Ritchey, A. D. Ekstrom, A. P. Yonelinas, C. Ranganath, CA1 and CA3 differentially support spontaneous retrieval of episodic contexts within human hippocampal subfields. *Nat. Commun.* **9**, 294 (2018).
23. T. Hainmueller, M. Bartos, Dentate gyrus circuits for encoding, retrieval and discrimination of episodic memories. *Nat. Rev. Neurosci.* **21**, 153–168 (2020).
24. T. Bartsch, J. Döhring, A. Rohr, O. Jansen, G. Deuschl, CA1 neurons in the human hippocampus are critical for autobiographical memory, mental time travel, and autonoetic consciousness. *Proc. Natl. Acad. Sci. U.S.A.* **108**, 17562–17567 (2011).
25. M. J. Kahana, Computational models of memory search. *Annu. Rev. Psychol.* **71**, 107–138 (2020).
26. J. R. Manning, M. R. Sperling, A. Sharan, E. A. Rosenberg, M. J. Kahana, Spontaneously reactivated patterns in frontal and temporal lobe predict semantic clustering during memory search. *J. Neurosci.* **32**, 8871–8878 (2012).
27. P. A. Yushkevich *et al.*, Automated volumetry and regional thickness analysis of hippocampal subfields and medial temporal cortical structures in mild cognitive impairment. *Hum. Brain Mapp.* **36**, 258–287 (2015).
28. B. B. Avants *et al.*, A reproducible evaluation of ANTs similarity metric performance in brain image registration. *Neuroimage* **54**, 2033–2044 (2011).
29. A. Klein, J. Tourville, 101 labeled brain images and a consistent human cortical labeling protocol. *Front. Neurosci.* **6**, 171 (2012).
30. M. W. Howard, M. J. Kahana, Contextual variability and serial position effects in free recall. *J. Exp. Psychol. Learn. Mem. Cogn.* **25**, 923–941 (1999).
31. N. M. Long *et al.*, Contextually mediated spontaneous retrieval is specific to the hippocampus. *Curr. Biol.* **27**, 1074–1079 (2017).
32. D. F. English *et al.*, Excitation and inhibition compete to control spiking during hippocampal ripples: Intracellular study in behaving mice. *J. Neurosci.* **34**, 16509–16517 (2014).
33. P. B. Sederberg, J. F. Miller, M. W. Howard, M. J. Kahana, The temporal contiguity effect predicts episodic memory performance. *Mem. Cognit.* **38**, 689–699 (2010).
34. C. T. Weidemann *et al.*, Neural activity reveals interactions between episodic and semantic memory systems during retrieval. *J. Exp. Psychol. Gen.* **148**, 1–12 (2019).
35. N. A. Herweg *et al.*, Reactivated spatial context guides episodic recall. *J. Neurosci.* **40**, 2119–2128 (2020).
36. N. M. Long, M. J. Kahana, Modulation of task demands suggests that semantic processing interferes with the formation of episodic associations. *J. Exp. Psychol. Learn. Mem. Cogn.* **43**, 167–176 (2017).
37. D. Sullivan *et al.*, Relationships between hippocampal sharp waves, ripples, and fast gamma oscillation: Influence of dentate and entorhinal cortical activity. *J. Neurosci.* **31**, 8605–8616 (2011).
38. E. Stark *et al.*, Pyramidal cell-interneuron interactions underlie hippocampal ripple oscillations. *Neuron* **83**, 467–480 (2014).
39. M. J. Kahana, *Foundations of Human Memory* (Oxford University Press, New York, 2012).
40. L. Tan, G. Ward, A recency-based account of the primacy effect in free recall. *J. Exp. Psychol. Learn. Mem. Cogn.* **26**, 1589–1625 (2000).
41. M. N. Shadlen, D. Shohamy, Decision making and sequential sampling from memory. *Neuron* **90**, 927–939 (2016).
42. A. Dubey, S. Ray, Cortical electrocorticogram (ECoG) is a local signal. *J. Neurosci.* **39**, 4299–4311 (2019).
43. A. J. Harding, G. M. Halliday, J. J. Kril, Variation in hippocampal neuron number with age and brain volume. *Cereb. Cortex* **8**, 710–718 (1998).
44. D. Keller, C. Erö, H. Markram, Cell densities in the mouse brain: A systematic review. *Front. Neuroanat.* **12** (2018).
45. J. Patel, E. W. Schomburg, A. Berényi, S. Fujisawa, G. Buzsáki, Local generation and propagation of ripples along the septotemporal axis of the hippocampus. *The J. Neurosci.* **33**, 17029–17041 (2013).
46. A. Jeneson, K. N. Mauldin, R. O. Hopkins, L. R. Squire, The role of the hippocampus in retaining relational information across short delays: The importance of memory load. *Learn. Mem.* **18**, 301–305 (2011).
47. J. F. Burke *et al.*, Theta and high-frequency activity mark spontaneous recall of episodic memories. *J. Neurosci.* **34**, 11355–11365 (2014).
48. P. B. Sederberg *et al.*, Hippocampal and neocortical gamma oscillations predict memory formation in humans. *Cereb. Cortex* **17**, 1190–1196 (2007).
49. J. J. Sakon, M. J. Kahana, Cognitive Electrophysiology Data Portal, Hippocampal ripples signal contextually-mediated episodic recall. https://memory.psych.upenn.edu/files/pubs/SakoKaha21.code.tgz. Deposited 6 June 2021.
50. J. N. Gelinas, D. Khodagholy, T. Thesen, O. Devinsky, G. Buzsáki, Interictal epileptiform discharges induce hippocampal-cortical coupling in temporal lobe epilepsy. *Nat. Med.* **22**, 641–648 (2016).
51. J. Sakon, M. J. Kahana, Data from "Human hippocampal ripples signal contextually mediated recall." Open Science Framework. https://osf.io/y5zwt. Deposited 18 January 2021.